Chapter 1

Introduction

Black Holes (BHs) are both extreme and ubiquitous objects which are increasingly becoming seen as central to our understanding of the physical universe. The first inferences of their existence came from the observations of the highly energetic Active Galactic Nucleus (AGN) Cygnus A as well as the rapid variability of quasars, both implying a massive and compact engine [e.g. **?**, and references therein]. Since then, the case for accretion onto a BH powering highly energetic events such as kiloparsec-scale jets and gamma ray bursts have strengthened considerably, however the mechanisms by which these observables are produced are still up for debate. There are also unconstrained questions regarding the nature of the event horizon and the surrounding space-time. The problem in these investigations is that there have been no direct observations which have resolved the innermost black hole emission on event horizon scales. However, this could change within the next few years as new generation of observatory comes into full operation.

1.1 Unsolved questions in black hole astrophysics

We will now provide the astrophysical motivation for this thesis through a discussion of several key questions in black hole astrophysics which could be constrained through observations which resolve the innermost emission region. Later in this chapter we present an upcoming network of telescopes which attempts to achieve this goal.

BHs are formed through the gravitational collapse of a stellar core during a supernovae explosion or from direct collapse from a primordial gas cloud and can grow in mass through accretion of nearby material and/or mergers with other black holes. The observed BH mass distribution is separated into two distinct mass classes, stellar and supermassive - the former with mass on the order $M \sim 10M_{\odot}$ and the latter $M \sim 10^{6} - 10^{10}M_{\odot}$ [Falcke and Markoff, 2013]. SMBHs form and reside (unless ejected) in the centres of all galaxies [**?**]. Observations of their surrounding galactic bulges show tight correlations between BH mass and both the bulge luminosity and stellar velocity dispersion [**??**], suggesting coevolution or feedback processes.

To constrain the physics near a black hole, the observation needs to be sensitive to scales comparable to the event horizon. For a non-spinning (Schwarschild) black hole, the event horizon is spherically symmetric with a radius,

$$R_{\rm Sch} = 2R_{\rm G} = 2GM_{\rm BH}/c^{2}, \tag{1.1}$$

where $R_{\rm G}$ is the Gravitational radius, $M_{\rm BH}$ is the black hole mass, G is the gravitational constant and c is the speed of light. The angular size of such an event horizon in the far-field approximation is

$$\theta_{\rm Sch} = R_{\rm Sch}/d_{\rm src} \tag{1.2}$$

$$\approx 0.02'' \times 10^{-9}(M_{\rm BH}/M_{\odot})({\rm kpc}/d_{\rm src}), \tag{1.3}$$

where $d_{\rm src}$ is the distance from observer to source.

Due it's size and proximity, the BH with the largest $\theta_{\rm Sch}$ turns out to be the SMBH in the centre of our own galaxy, Sgr A*. For Sgr A*, optical/infrared monitoring of orbiting stars [Gillessen et al., 2009] has yielded $M_{\rm BH} = 4.30 \pm 0.36 \times 10^6 M_\odot$ and $d_{\rm src} = 8.28 \pm 0.32$ kpc. Hence, for Sgr A*,

$$\theta_{\rm Sch} \approx 10'' \times 10^{-6}.$$

Innermost accretion and jet launch physics

[**I struggled to organise this subsection properly-suggestions welcome**] Accretion of gas onto the SMBH from large radii requires removal of both angular momentum and gravitational energy.

the innermost accretion disc result in the emission of highly energetic radiation as well as jets and wind outflows.

Theoretical and computational approaches are beginning to understand these processes however the range of scales needed to be simulated as well as uncertainties in the microphysics make a theoretical approach difficult.

The dominant emission mechanism for both accretion discs and jets is synchrotron radiation which is radiated by relativistic electrons spiralling in a magnetic field. Synchrotron sources typically exhibit a broad power-law spectrum and linearly polarised emission. The spectral energy distribution of Sgr A* peaks sharply in sub-millimetre, which for a self-absorbed synchrotron source implies that the emission becomes optically thin and at these frequencies,and that the emission arises from event horizon scales [Serabyn et al., 1997, Falcke et al., 1998]. Hence observations at the sub-millimetre are sensitive to the innermost emission. the orderedness of magnetic fields in the inner accretion disc and jet. Key discrimant for different jet launching models (see Johnson 2015b)

Radiatively Inefficient Accretion Flow [(RIAF), **??**] models offer a popular explanation for the $\sim 10^{-8} L_{\rm edd}$ of Sgr A*, however horizon scale obser-

vations are still needed to robustly compare models. In the RIAF model the electron and proton temperatures decouple due to the low density of the gas. Most of the gravitational energy is converted into the viscous thermal energy of protons which radiate inefficiently compared to electrons. The protons are then either advected into the SMBH or ejected via outflows possibly in the form of winds or a low powered jet. Currently we are still to determine whether the innermost emission of Sgr A* is disc or jet dominated.

In contrast, the powerful jet in M87 is thought to be powered by an accretion disc in the Magnetically Arrested Disc [(MAD), **?**] state, wherein accretion on the BH is suppressed by strong poloidal fields. ; the location of the jet base in M87 is in relation to its event horizon. M87 is on the other end of mass spectrum and has a very powerful jet.

differential rotation - source of energy, turns into MRI which can grow mag field and create turbulence Considering the physical processes around a BH as a black box scenario, accretion of gas onto a SMBH releases gravitational energy and angular momentum. Output from this process is radiation, jet and winds The classical idea of an Active Galactic Nucleus (AGN) is a SMBH surrounded by an accretion disc ejecting a jet along it's polar axis. The jets can remain collimate over large cosmic distances. magnetic fields Treating the system as a block box with parameters: M,a,$\dot{M}$,$L_{\rm edd}$, gas properties as large r.

fundamental plane of black hole activity - accretion rate and black hole mass seems to determine jet power however theory suggests that spin should power the jet (extracting the rotational energy from the black hole)

Measuring the black hole shadow

Fortunately, the innermost emission is gravitationally lensed by the SMBH, which causes it to appear magnified by several times its original size. In theory, the innermost orbit should be occupied by a ring of photons, the lensed image of which should feature a shadow-like (or 'silhouette') feature

[e.g. Johannsen and Psaltis, 2010]. Fig. 1.1 shows a cartoon illustration of the ray tracing combined with an early calculation of the ray-traced image of a thin accretion disc around a BH [**?**]. The circular shadow is apparent as the silhouette of the lensed emission originating from the far side of the disc.

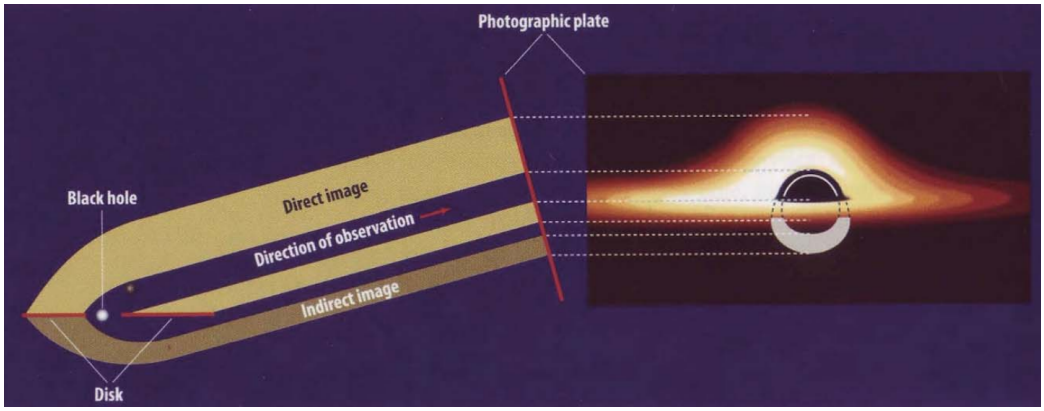

Figure 1.1: (Image credit : Shep Doeleman) Cartoon image (left) combined with the ray-tracing of a thin accretion disc surrounding a BH, first calculated by **?**. The cartoon image shows that both the bottom and top of the far side of the accretion disc is lensed by the black hole and is superimposed on the image of the near side of the accretion disc. The dark area in the centre, known as the black hole shadow is the lensed image of the photon ring orbiting the BH. A measurement of its precise shape is a test of general relativity in the strong field regime. Note that the left-right asymmetry in the image is due to doppler boosting.

Gravity as described by General Relativity (GR) is consistent with all observational experiments thus far [e.g. **?**], however GR has conceptual weaknesses, especially as it is not compatible with the quantum description of reality. Various alternatives to GR have been theorised which do not assume a purely classical description of matter. To compare GR with the alternatives, we have to compare its predictions in the strong, non-linear field regime where the largest deviations from GR would occur if it were an approximate theory.

The spacetime within several R_g around a SMBH provides such an oppor-

tunity. The precise shape of the photon ring around a SMBH is dependent on the spacetime which in turn is calculated within a theory of gravity [Takahashi, 2004]. The No-Hair theorem, which is based on GR, states that the spacetime should only be determined by the first two moments of the black hole, i.e. it's mass and spin. If the No-Hair theorem is invalid, the ring will deviate from a Schwarschild or Kerr profile. In the case of a non-zero quadrupole moment the ring will become either oblate or prolate [Johannsen and Psaltis, 2010].

1.2 Cranking up the angular resolution

Throughout the history of astronomy, there have been celestial sources which appear point-like (unresolved) with the available instrumentation. To investigate the nature of these sources, ever more sophisticated instruments with higher resolution are developed.

In principle, a diffraction-limited aperture can obtain an angular resolution of

$$\theta_{\rm res} \approx 1.22\ \lambda/D, \tag{1.4}$$

where D is the diameter of the aperture and λ is the observing wavelength. However, dish apertures larger than a hundred metres are infeasible to construct while systematic errors, including scattering-induced blurring due to inhomogeneous density (radio) or temperature (optical) distributions in the Earth's atmosphere can lead to instrument being unable to reach the diffraction limit. To overcome these difficulties and improve $\theta_{\rm res}$, a variety of new technologies have been developed (see Fig 1.2), including space-based observatories which escape the limitations set by the Earth's atmosphere, interferometric arrays which eliminate the need to build extremely large apertures, as well as technology-enabled mitigation strategies like adaptive optics and water vapour radiometry which account for atmospheric turbulence in real time.

The observing technique which typically achieves the highest angular resolution is Very Long Baseline Interferometry (VLBI). Interferometry refers to the technique of measuring the electric field correlations (named 'visibilities') between pairs of separated antennae. The visibilities are related to Fourier components on a section of approximately flat sky. Through an 'adequate' sampling of the Fourier domain an approximate image of sky can be reconstructed using the inverse Fourier transform. With this method, the distance between the antennae ($\boldsymbol{b}$, referred to as the 'baseline') effectively replaces D in equation 1.4, yielding a higher angular resolution than a single aperture. This technique is primarily used at radio frequencies while the electric field phase remains relatively stable. VLBI is essentially radio interferometry with antennae separated by large distances, typically $\gtrsim$ 100 km, including the possibility for antennae in Earth's orbit. A key distinction from connected-element interferometery is that independent clocks are needed at each station to facilitate the post-observation correlation. VLBI has seen several noteworthy achievements since its inception in the late 1960's, including resolution of the extra-galactic, compact, highly-variable objects, now known as quasars into super-luminal core-jet systems [e.g. **?**], and the mapping of maser motion around the Super-Massive Black Holes (SMBH) in the cores of nearby galaxies [e.g. **?**].

1.3 The Event Horizon Telescope

Overview

In the last few decades there has been a push to enhance VLBI capabilities at sub-millimetre wavelengths. One of the leading efforts in this regard is the Event Horizon Telescope consortium [(EHT), Doeleman et al., 2010], an international project whose primary objective is to spatially resolve the lensed photon rings of nearby SMBHs with an angular resolution on the order of their event horizons. In contrast to competing high frequency VLBI

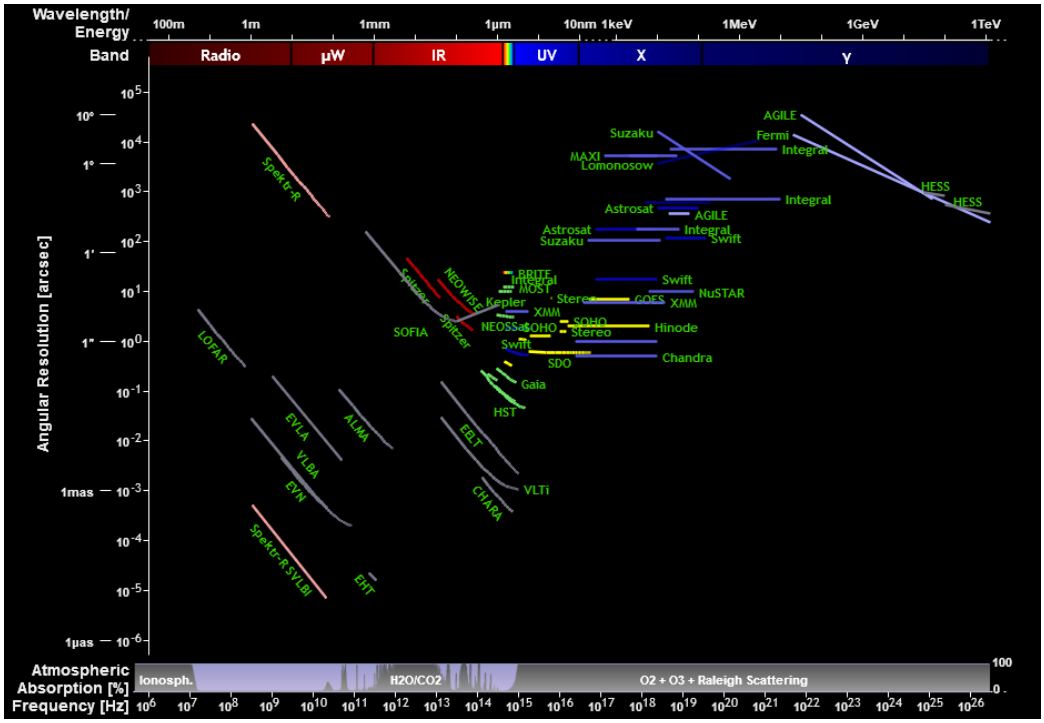

Figure 1.2: (Image credit: Olaf Frohn[2]) An illustration of angular resolution vs. observing frequency across the entire observational spectrum, shown for a selection of observatories. The VLBI arrays : Spektr-R SVLBI (or RadioAstron) and the EHT clearly achieve the highest angular resolution of all due to their long baselines. At the bottom of the plot, there is a panel showing atmospheric/ionospheric absorption as a function of wavelength, and consequently all observatories in the zero transmission zones are space-based.

observatories e.g. the Very Long Baseline Array (VLBA) which has coverage to 87 GHz (3 mm), the EHT is operating at 230 GHz (1.3 mm) and will potentially extend till 345 GHz (0.8 mm) in the future. See Fig. 1.3 for an annotated map of the locations of the EHT array. As the EHT will have baseline lengths comparable to the diameter of the earth, $|b| \sim 10^4$ km and is operating at 1.3 mm, this yields $\theta_{\rm res} \sim 30$ μ-arcsec. The two primary targets Sgr A* and M87 are expected to have gravitationally-lensed photon

rings with apparent angular diameters of $\theta_{\rm pr} \sim 50$ and $\sim 20 - 40$ μ-arcsec respectively [Broderick and Loeb, 2009, Falcke and Markoff, 2013], and hence should be resolvable by the EHT.

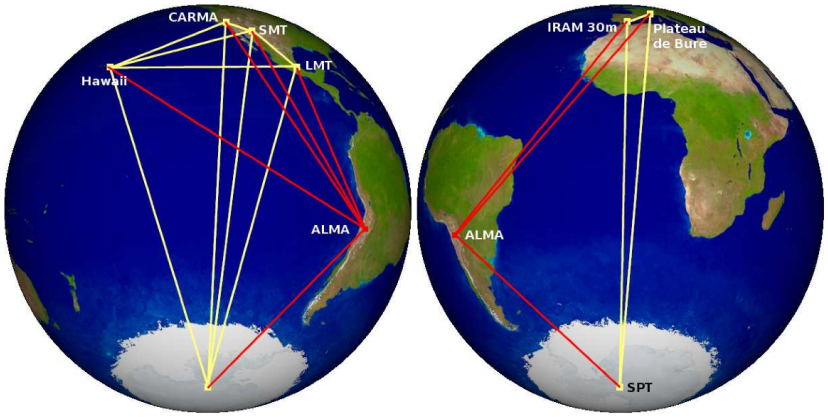

Figure 1.3: (Image credit: Remo Tilanus) The view of the Event Horizon Telescope (EHT) from Sgr A*. This interferometric array uses Earth-diameter baselines, operating at 230−345 GHz to attain an angular resolution of the order of $\theta_{\rm res} \sim 10$ μ-arcsec. Baselines to ALMA are shown in red, to highlight its order of magnitude higher sensitivity. Note that the CARMA station has recently been decommissioned, a telescope in Greenland is currently being constructed and there is ongoing investigation into a possible site on the African continent.

Instrumentation and observational challenges

The development of mm-VLBI instrumentation has been spurred by the formation of EHT as a project and the deepening of theory and simulation work over the past two decades. This is evidenced by the comparable observational results but starkly different interpretations of Krichbaum et al. [1998] and Doeleman et al. [2008]. A decade apart, both teams observed Sgr A* with a mm-VLBI arrays consisting of three stations at similar frequency (215 GHz in 1998 and 230 GHz in 2008). Although the former was limited by calibration uncertainties, the primary difference in analysis and interpretation was

that the latter result was linked explicitly to the innermost accretion physics in the event horizon region [e.g. Broderick et al., 2011]. In this way, the newly developed theoretical context contributed to the significance of the Doeleman et al. [2008] result. However, a robust comparison with this diverse body of theoretical work would require a significant leap in mm-VLBI observational capabilities. For example, to discern whether the No-Hair theorem is violated requires the fractional asymmetry of the shadow shape with respect to its angular size to be measured to a few percent [e.g. Goddi et al., 2016, and references therein]. To achieve this level of precision, the development of the global mm-VLBI array will face significant challenges.

The move to higher frequencies is accompanied by requirements on the instrument including: increased data rates ($1 \rightarrow 16$ GHz) and stability of timing standards; as well as increased accuracy of dish surfaces and antenna pointing accuracy. Difficulties emerge also from the effects of the Earth's lower atmosphere where optical depth becomes significant and turbulence causes rapid fluctuations in the signal transmission time which causes decoherence in the visibilities. Even though the stations are at high altitude, desert locations, the atmospheric coherence times are still short, typically $\lesssim$10 s [Doeleman et al., 2009]. The extensive requirements on instruments and location drive up the cost of mm-VLBI stations, resulting in few element (< 10) interferometric arrays which make for sparse sampling of the Fourier domain. This is exacerbated by short mutual visibility windows and imperfect weather. Traditional phase referencing calibration is ruled out due to the variable atmosphere, the low sub-mm source density and that calibrators are resolved and variable too at this high angular resolution.

Aside from the considerations listed above, there is a string of complications relating to the sources, the ISM and the calibration procedure. Firstly the emission from the primary source, Sgr A*, is strongly scattered by turbulent electron plasma in the Interstellar Medium (ISM) along this line-of-sight. This results in a Gaussian-blurring effect [see Fig. **??**, e.g. Fish et al.,

2014] which falls as ν^{-2} and become subdominant to intrinsic structure in the sub-millimetre range. This medium both blurs and introduces random, time-variable substructure into the source brightness distribution (see section **??**). The scattering substructure adds complications for data interpretation as its contribution is difficult to disentangle from that of the intrinsic source sub-structure, depending on the time-scale of the observation. also mention that the effects of synchrotron self-absorption and optically thick/thiness The second issue is that the source is intrinsically variable over minutes to hours (see section **??**). The fact that the source is variable over the course of a single observation epoch breaks a fundamental assumption in interferometry as the visibilities cannot be related to a static sky image. This (broken) assumption is central to technique of self-calibration (see section **??**), while in fact both the source and the ISM are time-variable.

These effects, among others, may place significant limitations on the sensitivity, image fidelity, and dynamic range that can be achieved with mm-VLBI observations [Blecher et al., 2016]. Furthermore, unaccounted for systematic and/or non-Gaussian uncertainties could preclude robust, accurate Bayesian parameter estimation and model selection analyses of accretion flow [e.g. Broderick et al., 2016] and gravitational physics [e.g. Broderick et al., 2014, Psaltis et al., 2016], two of the EHT's many objectives. It is therefore imperative that a deep, quantified understanding of mm-VLBI's ability to measure and discern between theoretical predictions in the presence of a myriad of signal corruptions.

1.4 A realistic mm-VLBI simulator

Given the significant observational challenges that the EHT faces, we have undertaken this project to build a mm-VLBI observation and signal corruption simulator. There are many benefits for using such a toolkit and indeed synthetic data simulation is common practice for major scientific experi-

ments. A prominent example is the extensive gravitational wave template matching scheme for The Laser Interferometer Gravitational-Wave Observatory (LIGO) which operates in the presence of tidal loading, passing trains etc. In essence such a simulator would fill in the final component of the theoretical signal propagation chain, effectively taking astrophysical simulations of the source (e.g. accretion onto a SMBH) as an input and returning realistic synthetic interferometric data. This allows a more effective interplay between theory and observation, quantifying systematic effects and the measurement limits. The remainder of this section will briefly discuss several research questions relevant to an EHT synthetic data simulator and how we approach the software design in order to address these questions.

A key use case for simulated data is the testing of calibration, parameter estimation and imaging algorithms and strategies. As the inputs to the simulator are known exactly, we are better able to explore sources of error which are difficult to disentangle from intrinsic source features when using only real data. A straightforward way to perform such a test is through the creation of a set of 'standard challenge' dataset. Such datasets would be available to the entire community to input into their calibration and/or imaging routines. Following this, a detailed comparison between the different strategies in varying regimes (source, ISM, troposphere and instrumental) can be made. Importantly, a systematic investigation of a particular algorithm across many different datasets could provide insight into subtle or previously unknowns sources of error inherent in that routine.

Simulated data can also assist in the optimisation of the experimental configuration. Financial constraints require the prioritisation of hardware upgrades e.g. increasing bandwidth, surface accuracy improvement, deployment of water vapour radiometers or additional receiver bands. Simulated data together with calibration and imaging pipelines can help to quantify the benefit of each improvement based on expected scientific return in units of precision of the scientific parameter of interest (e.g. shadow assymetry)

rather than more generic terms (e.g. angular resolution, positional uncertainty) that may not have an associated systematic effect included. This approach can even be extended to assess new candidate stations, especially as new geographic locations (e.g. in Southern Africa) are receiving increasing attention due to the potential long baselines to ALMA, SPT and European stations.

"Recently, there has been an increase in the attention given to simulating EHT observations of Sgr A* and M87 [Fish et al., 2014, Lu et al., 2014, Bouman et al., 2015, Lu et al., 2016, Chael et al., 2016]. However, these are primarily focused on image reconstruction and assume either negligible or Gaussian distributed gain errors; perfect antenna pointing accuracy; and in most cases only Gaussian convolution to simulate ISM scattering. Clearly, as the EHT array is enhanced (and possibly expanded), so too must the interferometric simulations evolve to provide ever-more physical predictions on the confidence levels with which parameters can be extracted and hence exclude theoretical models of gravity and/or accretion flows.

Over the past decade, significant effort has been placed on advanced radio interferometric calibration and imaging algorithms for centimetre and metre-wave facilities in response to the large number of new arrays in construction or design phase (e.g. MeerKAT, ASKAP, SKA, LOFAR, HERA). A leading software package in this pursuit is MeqTrees[3] [Noordam and Smirnov, 2010], which was developed to simulate, understand and address the calibration issues to be faced with the greatly enhanced sensitivity, instantaneous bandwidth, and field-of-view of such facilities. For example, MeqTrees is rooted in the Measurement Equation mathematical formalism [Hamaker et al., 1996], which parameterizes the signal path into distinct 2×2 complex matrices called Jones matrices. This formalism and applications thereof are laid out in [Smirnov, 2011a,b,c] and are arbitrarily generalized to model any (linear) effect, including undesired signal corruptions that often may

[3]https://ska-sa.github.io/meqtrees/

have subtle yet systematic effects. MeqTrees has been applied to correct for direction-dependent calibration errors to Karl. G. Jansky Very Large Array (VLA) and Westerbork Synthesis Radio Telescope (WSRT) observations, achieving record-breaking high dynamic range images [Smirnov, 2011c, Makhathini et al, in prep.]. The effectiveness provided by the Measurement Equation formalism in radio interferometric calibration provides a strong motivation to explore its application to the challenging goal of imaging a supermassive black hole silhouette with mm-VLBI. To construct this simulator we leverage off metre and cm-wavelength simulation and calibration successes and build a MeqTrees-based mm-VLBI-specific software package which we name, MeqSilhouette. Use of MeqTrees and measurement set data format lends itself to investigating a range of different techniques that are used in other areas of interferometry [e.g. **?**]. While MeqTrees has not yet been used in the context of mm-wavelength observations, the framework is agnostic to higher frequency implementation as long as the Measurement Equation is appropriately constructed." [Blecher et al., 2016]

1.5 Outline

This thesis is broadly divided into the following chapters and sections,

- **Chapter 2 : Theory**

  Section 2.1 introduces radio interferometry via the Measurement Equation formalism, followed by mm-VLBI tailored discussions on calibration, data products and the consequences of breaking the static source assumption.

  Section 2.2 is a review and investigation into the key signal corruptions implemented in the meqsilhouette simulator i.e. instrumentation imperfections and transmission through the ISM and Earth's atmosphere.

- **Chapter 3 : Software Implementation**

  Section 3.1 summarises the key software design objectives considered.

  Section 3.2 is a description of the design and construction of the simulation software with emphasis on the software architechure and workflow.

- **Chapter 4 : Results**

  Section 4.1 showcases the basics of the simulator output through a series of canonical results.

  Section 4.2 presents a more sophisticated scenario which tests an AIPS calibration routine in the presence of source and tropospheric time-variability.

- **Chapter 5 : Discussion**

  Section 5.1 explores the implications of the results shown in the previous chapter.

  Section 5.2 makes suggestions for future applications of and improvements to the simulator.

- **Chapter 6 : Conclusions**
  We summarise the work and context of this thesis.

Bibliography

T. Blecher, R. Deane, G. Bernardi, and O. Smirnov. MeqSilhouette : A mm-VLBI observation and signal corruption simulator. *ArXiv e-prints*, August 2016.

K. L. Bouman, M. D. Johnson, D. Zoran, V. L. Fish, S. S. Doeleman, and W. T. Freeman. Computational Imaging for VLBI Image Reconstruction. *ArXiv e-prints*, dec 2015.

A. E. Broderick, V. L. Fish, S. S. Doeleman, and A. Loeb. Constraining the Structure of Sagittarius A*'s Accretion Flow with Millimeter Very Long Baseline Interferometry Closure Phases. ApJ, 738:38, September 2011. doi: 10.1088/0004-637X/738/1/38.

Avery E. Broderick and Abraham Loeb. IMAGING THE BLACK HOLE SILHOUETTE OF M87: IMPLICATIONS FOR JET FORMATION AND BLACK HOLE SPIN. *ApJ*, 697(2):1164–1179, may 2009. doi: 10.1088/0004-637x/697/2/1164. URL `http://dx.doi.org/10.1088/0004-637x/697/2/1164`.

Avery E. Broderick, Tim Johannsen, Abraham Loeb, and Dimitrios Psaltis. TESTING THE NO-HAIR THEOREM WITH EVENT HORIZON TELESCOPE OBSERVATIONS OF SAGITTARIUS A*. *ApJ*, 784 (1):7, feb 2014. doi: 10.1088/0004-637x/784/1/7. URL `http://dx.doi.org/10.1088/0004-637x/784/1/7`.

Avery E. Broderick, Vincent L. Fish, Michael D. Johnson, Katherine Rosenfeld, Carlos Wang, Sheperd S. Doeleman, Kazunori Akiyama, Tim Johannsen, and Alan L. Roy. MODELING SEVEN YEARS OF EVENT HORIZON TELESCOPE OBSERVATIONS WITH RADIATIVELY INEFFICIENT ACCRETION FLOW MODELS. *ApJ*, 820(2):137, mar 2016. doi: 10.3847/0004-637x/820/2/137. URL `http://dx.doi.org/10.3847/0004-637x/820/2/137`.

A. A. Chael, M. D. Johnson, R. Narayan, S. S. Doeleman, J. F. C. Wardle, and K. L. Bouman. High Resolution Linear Polarimetric Imaging for the Event Horizon Telescope. *ArXiv e-prints*, May 2016.

S. Doeleman, E. Agol, D. Backer, F. Baganoff, G. C. Bower, A. Broderick, A. Fabian, V. Fish, C. Gammie, P. Ho, M. Honman, T. Krichbaum, A. Loeb, D. Marrone, M. Reid, A. Rogers, I. Shapiro, P. Strittmatter, R. Tilanus, J. Weintroub, A. Whitney, M. Wright, and L. Ziurys. Imaging an Event Horizon: submm-VLBI of a Super Massive Black Hole. In *astro2010: The Astronomy and Astrophysics Decadal Survey*, volume 2010 of *Astronomy*, 2010.

Sheperd S. Doeleman, Jonathan Weintroub, Alan E. E. Rogers, Richard Plambeck, Robert Freund, Remo P. J. Tilanus, Per Friberg, Lucy M. Ziurys, James M. Moran, Brian Corey, Ken H. Young, Daniel L. Smythe, Michael Titus, Daniel P. Marrone, Roger J. Cappallo, Douglas C.-J. Bock, Geoffrey C. Bower, Richard Chamberlin, Gary R. Davis, Thomas P. Krichbaum, James Lamb, Holly Maness, Arthur E. Niell, Alan Roy, Peter Strittmatter, Daniel Werthimer, Alan R. Whitney, and David Woody. Event-horizon-scale structure in the supermassive black hole candidate at the Galactic Centre. *Nature*, 455(7209):78–80, sep 2008. doi: 10.1038/nature07245. URL `http://dx.doi.org/10.1038/nature07245`.

Sheperd S. Doeleman, Vincent L. Fish, Avery E. Broderick, Abraham Loeb, and Alan E. E. Rogers. DETECTING FLARING STRUCTURES IN

SAGITTARIUS A* WITH HIGH-FREQUENCY VLBI. *ApJ*, 695(1):59–74, mar 2009. doi: 10.1088/0004-637x/695/1/59. URL http://dx.doi.org/10.1088/0004-637x/695/1/59.

H Falcke and S B Markoff. Toward the event horizon—the supermassive black hole in the Galactic Center. *Class. Quantum Grav.*, 30(24):244003, nov 2013. doi: 10.1088/0264-9381/30/24/244003. URL http://dx.doi.org/10.1088/0264-9381/30/24/244003.

Heino Falcke, W. M. Goss, Hiroshi Matsuo, Peter Teuben, Jun-Hui Zhao, and Robert Zylka. The Simultaneous Spectrum of Sagittarius A* from 20 Centimeters to 1 Millimeter and the Nature of the Millimeter Excess. *ApJ*, 499(2):731–734, jun 1998. doi: 10.1086/305687. URL http://dx.doi.org/10.1086/305687.

Vincent L. Fish, Michael D. Johnson, Ru-Sen Lu, Sheperd S. Doeleman, Katherine L. Bouman, Daniel Zoran, William T. Freeman, Dimitrios Psaltis, Ramesh Narayan, Victor Pankratius, Avery E. Broderick, Carl R. Gwinn, and Laura E. Vertatschitsch. IMAGING AN EVENT HORIZON: MITIGATION OF SCATTERING TOWARD SAGITTARIUS A*. *ApJ*, 795(2):134, oct 2014. doi: 10.1088/0004-637x/795/2/134. URL http://dx.doi.org/10.1088/0004-637x/795/2/134.

S. Gillessen, F. Eisenhauer, T. K. Fritz, H. Bartko, K. Dodds-Eden, O. Pfuhl, T. Ott, and R. Genzel. The Orbit of the Star S2 Around SGR A* from Very Large Telescope and Keck Data. ApJ, 707:L114–L117, December 2009. doi: 10.1088/0004-637X/707/2/L114.

C. Goddi, H. Falcke, M. Kramer, L. Rezzolla, C. Brinkerink, T. Bronzwaer, R. Deane, M. De Laurentis, G. Desvignes, J. R. J. Davelaar, F. Eisenhauer, R. Eatough, R. Fraga-Encinas, C. M. Fromm, S. Gillessen, A. Grenzebach, S. Issaoun, M. Janßen, R. Konoplya, T. P. Krichbaum, R. Laing, K. Liu, R.-S. Lu, Y. Mizuno, M. Moscibrodzka, C. Müller, H. Olivares, O. Porth,

O. Pfuhl, E. Ros, F. Roelofs, K. Schuster, R. Tilanus, P. Torne, I. van Bemmel, H. J. van Langevelde, N. Wex, Z. Younsi, and A. Zhidenko. BlackHoleCam: fundamental physics of the Galactic center. *ArXiv e-prints*, June 2016.

J. P. Hamaker, J. D. Bregman, and R. J. Sault. Understanding radio polarimetry. I. Mathematical foundations. A&AS, 117:137–147, May 1996.

T. Johannsen and D. Psaltis. Testing the No-hair Theorem with Observations in the Electromagnetic Spectrum. II. Black Hole Images. ApJ, 718:446–454, July 2010. doi: 10.1088/0004-637X/718/1/446.

T. P. Krichbaum, D. A. Graham, A. Witzel, A. Greve, J. E. Wink, M. Grewing, F. Colomer, P. de Vicente, J. Gomez-Gonzalez, A. Baudry, and J. A. Zensus. VLBI observations of the galactic center source SGR A* at 86 GHz and 215 GHz. A&A, 335:L106–L110, July 1998.

R.-S. Lu, F. Roelofs, V. L. Fish, H. Shiokawa, S. S. Doeleman, C. F. Gammie, H. Falcke, T. P. Krichbaum, and J. A. Zensus. Imaging an Event Horizon: Mitigation of Source Variability of Sagittarius A*. ApJ, 817:173, February 2016. doi: 10.3847/0004-637X/817/2/173.

Ru-Sen Lu, Avery E. Broderick, Fabien Baron, John D. Monnier, Vincent L. Fish, Sheperd S. Doeleman, and Victor Pankratius. IMAGING THE SUPERMASSIVE BLACK HOLE SHADOW AND JET BASE OF M87 WITH THE EVENT HORIZON TELESCOPE. *ApJ*, 788(2):120, may 2014. doi: 10.1088/0004-637x/788/2/120. URL `http://dx.doi.org/10.1088/0004-637x/788/2/120`.

M. Mościbrodzka, H. Falcke, H. Shiokawa, and C. F. Gammie. Observational appearance of inefficient accretion flows and jets in 3D GRMHD simulations: Application to Sagittarius A*. A&A, 570:A7, October 2014. doi: 10.1051/0004-6361/201424358.

J. E. Noordam and O. M. Smirnov. The MeqTrees software system and its use for third-generation calibration of radio interferometers. A&A, 524: A61, nov 2010. doi: 10.1051/0004-6361/201015013. URL http://dx.doi.org/10.1051/0004-6361/201015013.

Dimitrios Psaltis, Norbert Wex, and Michael Kramer. A QUANTITATIVE TEST OF THE NO-HAIR THEOREM WITH Sgr A* USING STARS PULSARS AND THE EVENT HORIZON TELESCOPE. *ApJ*, 818(2): 121, feb 2016. doi: 10.3847/0004-637x/818/2/121. URL http://dx.doi.org/10.3847/0004-637x/818/2/121.

E. Serabyn, J. Carlstrom, O. Lay, D. C. Lis, T. R. Hunter, J. H. Lacy, and R. E. Hills. High-Frequency Measurements of the Spectrum of Sagittarius A*. *ApJ*, 490(1):L77–L81, nov 1997. doi: 10.1086/311010. URL http://dx.doi.org/10.1086/311010.

O. M. Smirnov. Revisiting the radio interferometer measurement equation. *A&A*, 527:A106, 2011a. doi: 10.1051/0004-6361/201016082. URL http://dx.doi.org/10.1051/0004-6361/201016082.

O. M. Smirnov. Revisiting the radio interferometer measurement equation. *A&A*, 527:A107, 2011b. doi: 10.1051/0004-6361/201116434. URL http://dx.doi.org/10.1051/0004-6361/201116434.

O. M. Smirnov. Revisiting the radio interferometer measurement equation. *A&A*, 527:A108, 2011c. doi: 10.1051/0004-6361/201116435. URL http://dx.doi.org/10.1051/0004-6361/201116435.

R. Takahashi. Shapes and Positions of Black Hole Shadows in Accretion Disks and Spin Parameters of Black Holes. ApJ, 611:996–1004, August 2004. doi: 10.1086/422403.